Available online at www.sciencedirect.com
SCIENCE DIRECT
Energy and Buildings 38 (2006) 1200–1211
ENERGY and BUILDINGS
www.elsevier.com/locate/enbuild

Parametric space distribution effects of wall heat capacity and thermal resistance on the dynamic thermal behavior of walls and structures

P.T. Tsilingiris

Department of Energy Engineering, Technological Education Institution (TEI) of Athens, A. Spyridonos Str., GR 12210 Egaleo, Athens, Greece

Received 28 October 2005; received in revised form 20 January 2006; accepted 18 February 2006

Abstract

The present work aims at the investigation of the combined space distribution effects of heat capacity and thermal resistance on the transient thermal behavior of a wall, seen as a continuum of distributed parameters. The physical system is compared with the idealized wall lumped parameter model and its thermal time constant is related to its effective wall heat capacity, defined as the fraction of the wall heat capacity which participates in a transient thermal process. The effect of the space distribution of heat capacity and thermal resistance on the effective wall heat capacity is investigated for a wide range of homogeneous and multilayer thermally insulated walls. It is derived that the decrease of thermal resistance in homogeneous walls leads to an increase of their effective heat capacity. However, the effects are remarkably stronger on the effective heat capacity of thermally insulated multilayer walls, in which when the thermal insulation layer is at the ambient side, it leads to a significant increase of effective heat capacity, although when it is installed at the room side it leads to very low effective heat capacity, irrespective of the wall thermal resistance. Based on the first order results from a simplified room model, it was subsequently found that the influence of these parameters on the effective heat capacity of the building envelope leads to significant effects on the transient thermal behavior, thermal time constant and stability of structures.

Keywords: Lumped heat capacity; Distributed heat capacity; Time constant; Effective heat capacity; Thermal stability

1. Introduction

The importance of the building envelope has long been established as a technology which is vital for the development of indoor comfort conditions, leading to a substantial energy conservation and drastic operational cost reduction of the employed H-V-A-C systems in buildings, with obviously favorable environmental influences. Towards this aim a substantial research work, both theoretical and experimental, has been carried out aiming at the investigation of the transient thermal behavior of walls based mainly on response function with formulation allowing transformation in the frequency domain [1–3], Fourier transform [4] and numerical methods [5–7]. The potential of significant energy savings with large heat capacity instead of lightweight walls of comparable thermal resistance was noticed by Christian and Kosny [8], who suggested the development of new dynamic procedures for the evaluation of wall performance. It has been recently proposed that wall thermal time constant (forward, F or reverse R) may be proved to be an important quantity for the dynamic wall performance evaluation [9]. The significance of the heat capacity and thermal resistance distribution along the thickness of a plane wall was noticed by Kossecka and Kosny [10], who developed and correlated the dimensionless thermal structure factors with wall response factors. They also investigated the effect of wall thermal insulation configuration which determines the thermal structure factors on the wall frequency response and on heating and cooling loads of a building [11]. Significant amount of research work has also been carried out towards the thermal modeling and characterization of their transient thermal behavior and the evaluation of their time constant, based on in situ actual measurements in buildings [12–15] as well as on physical system component modeling based on numerical analysis or frequency domain methods [16–18]. Significant effects of the space distribution of heat capacity on the transient wall thermal behavior were previously derived, under the influence of step temperature change excitations [9]. According to more recent investigations, it has been found that although the space distribution of heat capacity does not affect the quasi-steady state

E-mail address: ptsiling@teiath.gr.

0378-7788/$ – see front matter © 2006 Elsevier B.V. All rights reserved.
doi:10.1016/j.enbuild.2006.02.007

Nomenclature

A	area (m^2)
Bi	Biot number
c	specific heat capacity (J/(kg K))
C	heat capacity (J/K)
h	convective heat transfer coefficient (W/(m^2 K))
HCA	per unit surface area heat capacity (J/(m^2 K))
k	thermal conductivity (W/(m K))
K	numerical constant
L	wall thickness (m)
m	mass (kg)
n	number of homogeneous layers
N	number of slices
p	number of time increments Δt
q	heat flux rate (W/m^2)
$\bar{q}$	average heat flux rate (W/m^2)
r	slice element thermal resistance (K/W)
R	thermal resistance (K/W)
t	time (s)
T	temperature (°C)
$\bar{T}$	average temperature (°C)
TC	time constant (s)
x	space coordinate (m)

Greek letters

δ	layer thickness (m)
Δ	difference
ξ	heat capacity ratio
ρ	density (kg/m^3)
φ	phase angle (°)

Subscripts

a	air
b	brick
c	concrete
d	domain
eff	effective
F	forward
is	slice value
n	net
o	indoor
R	reverse
w	wall
wi	wall initial
∞	ambient

wall thermal behavior for a wide range of heat capacities, there is a remarkably strong effect of space distribution of heat capacity on the transient response of a multilayer wall under the effect of harmonically time varying environmental forcing functions [19]. The aim of the present work is the investigation of the physical significance and the evaluation of parametric effects of the space distribution of heat capacity across the distributed thermal resistance of a wall, at a direction perpendicular to its plane, on the way it responds as a distributed continuum to thermal excitations corresponding to a step temperature change. This behavior which determines the wall thermal time constant is employed for the evaluation of the fraction of the system heat capacity, which is involved with the transient thermal process and is known as effective wall heat capacity. This quantity, which is not restrictive only to vertical but is also extended to horizontal structural elements of the building envelope, is compared to the idealized situation when the thermal resistance of the heat flow path diminishes to an infinitely small value, which corresponds to concentrated heat capacity systems. The significant implication of this important parameter of the building envelope on the time constant and the thermal stability of structures is further investigated, using a simplified test room model analysis.

2. The dynamic modeling of building components

The dynamic thermal behavior of the building envelope which affects considerably the thermal performance of structures is associated with various physical and design parameters like heat capacity, thermal resistance and also their space distribution at the direction of the heat flow path. Although the building components such as walls or ceilings may sometimes exhibit strongly three-dimensional effects owing to various imperfections or presence of thermal bridges, studs or corners, their effects can be neglected allowing simple one-dimensional approach, without affecting the significance of the basic physical model. Therefore, the wall can be modeled as a one-dimensional continuum of a single or several homogenous layers in thermal contact. The wall heat capacity for a homogenous wall is defined as the product of wall mass multiplied by its specific heat capacity while in the case of a composite wall with n homogenous layers of mass m_i and a specific heat capacity c_i is defined as,

$$C = \sum_{i=1}^{n} m_i c_i \tag{1}$$

Usually, instead of the previous quantity, the per unit wall surface area heat capacity (J/(m^2 K)) is employed, defined as

$$\mathrm{HCA} = \frac{C}{A} = \sum_{i=1}^{n} \rho_i \cdot c_i \cdot \delta_i \tag{2}$$

where ρ_i and δ_i are the wall layer density and thickness, respectively.

During dynamic processes, the wall temperature may under certain conditions remain essentially uniform. According to the fundamental theory [20], this occurs for an adequately small value of the dimensionless Biot number, which being defined as,

$$Bi = \frac{h \cdot L_c}{k} \leq 0.1 \tag{3}$$

determines the relative influence of heat conduction to convection resistance within the wall, with h the convective heat transfer coefficient at wall boundaries, k the thermal conductivity and L_c a characteristic length which for a homogenous layer material corresponds to the wall thickness. When the condition (3) is satisfied the wall can be treated as a lumped

parameter model, something which leads to significant simplifications in the analysis of the transient phenomena.

2.1. The lumped parameter wall model

Assume that the condition (3) is satisfied for a homogeneous wall, which at $t = t_0$ is placed between a room space at the fixed temperature T_o and the environment at the temperature T_∞. Under these conditions, the time dependent wall temperature remains essentially uniform and therefore it can be considered as a single node lumped parameter model as is shown in Fig. 1a. This occurs for a negligibly small wall thermal resistance, so the wall heat capacity C at the node W is connected to the ambient and room temperature nodes T_∞ and T_o by the corresponding film resistances $R_\infty = 1/(h_\infty A)$ and $R_o = 1/(h_o \cdot A)$, respectively.

The heat balance equation at the node W then yields,

$$m_w \cdot c_w \cdot [T_w(t) + dT_w - T_\infty] - m_w \cdot c_w \cdot [T_w(t) - T_\infty] = h_o \cdot A \cdot [T_o - T_w(t)]\,dt - h_\infty \cdot A \cdot [T_w(t) - T_\infty)]\,dt \quad (4)$$

Assuming that the lumped wall heat capacity is $C = m_w \cdot c_w$, the time dependent phenomenon is governed by the following differential equation which is derived by the rearrangement of the previous expression:

$$\frac{d[T_w(t) - T_\infty]}{dt} + \frac{A \cdot (h_o + h_\infty)}{C} \cdot [T_w(t) - T_\infty] = \frac{h_o \cdot A}{C} \cdot (T_o - T_\infty) \quad (5)$$

The solution of the previous equation is,

$$[T_w(t) - T_\infty] \cdot \exp\left[\frac{A \cdot (h_o + h_\infty)}{C}\right] \cdot t = \frac{h_o \cdot (T_o - T_\infty)}{h_o + h_\infty} \cdot \exp\left[\frac{A \cdot (h_o + h_\infty)}{C}\right] \cdot t + K \quad (6)$$

with the integration constant K derived by the initial condition of the problem which is that at $t = 0$ the wall temperature is at the uniform temperature $T_w(0) = T_{wi}$.

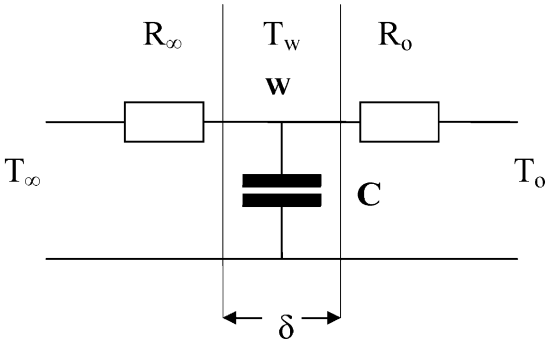

WALL

(a)

k, ρ, c

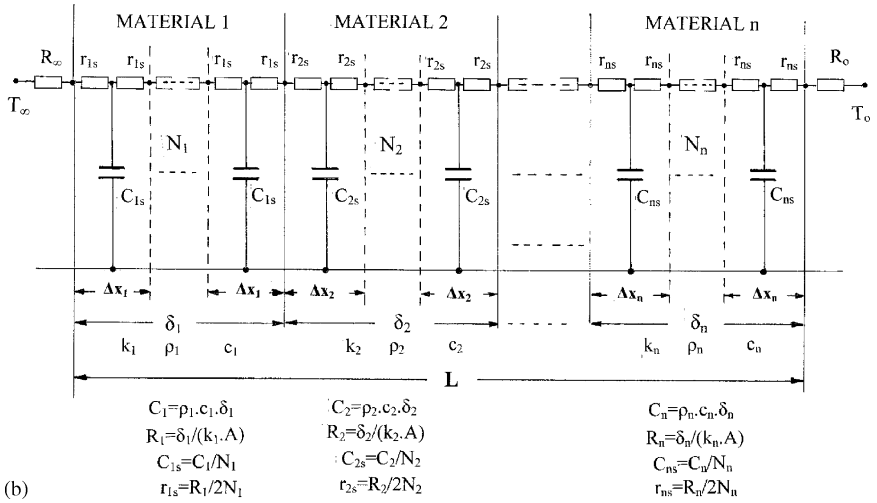

(b)

Fig. 1. (a) The homogenous wall with thermophysical properties k, ρ and c as a lumped parameter model. (b) The multilayer wall of distributed parameters, consisting of n homogenous layers of thickness δ_i, with thermophysical properties k_i, ρ_i and c_i, $1 \le i \le n$.

Substitution of its value in (6) yields,

$$T_w(t) - T_\infty = \frac{h_o}{h_o + h_\infty} \cdot (T_o - T_\infty) + \left[T_{wi} - T_\infty - \frac{h_o}{h_o + h_\infty} \cdot (T_o - T_\infty) \right] \cdot \exp\left[- \frac{A \cdot (h_o + h_\infty)}{C} \right] \cdot t \quad (7)$$

Since,

$$T_w(t) - T_\infty = (T_o - T_\infty) - [T_o - T_w(t)] \quad (8)$$

$$T_{wi} - T_\infty = (T_o - T_\infty) - (T_o - T_{wi}) \quad (9)$$

it is derived from (7) that,

$$T_o - T_w(t) = (T_o - T_\infty) \cdot \left[\frac{h_\infty}{h_o + h_\infty} - \left(\frac{h_\infty}{h_o + h_\infty} - \frac{T_o - T_{wi}}{T_o - T_\infty} \right) \cdot \exp\left[- \frac{A \cdot (h_o + h_\infty)}{C} \cdot t \right] \right] \quad (10)$$

The previous expression can then be employed for the calculation of the time dependent heat flux at the room side of the wall, which is derived by the following expression:

$$q_o(t) = h_o \cdot (T_o - T_\infty) \cdot \left[\frac{h_\infty}{h_o + h_\infty} - \left(\frac{h_\infty}{h_o + h_\infty} - \frac{T_o - T_{wi}}{T_o - T_\infty} \right) \cdot \exp\left[- \frac{A \cdot (h_o + h_\infty)}{C} \cdot t \right] \right] \quad (11)$$

According to the previous exponential expression, the maximum heat flux which is developed at $t = 0$ is,

$$q_o(0) = h_o \cdot (T_o - T_{wi}) \quad (12)$$

which, as $t \to \infty$, decreases exponentially to its asymptotic steady state value of

$$q_o(t) = \bar{q}_o = \frac{h_o \cdot h_\infty}{h_o + h_\infty} \cdot (T_o - T_\infty) \quad (13)$$

The multiplication factor of the temperature difference term in the right hand side of the previous expression denotes that for a given wall boundary temperature difference, the steady state heat flux for the developed lumped heat capacity model is dominated by the wall film conductances.

The following quantity which appears between brackets at the exponent of the right hand side of expression (11) is defined as the wall time constant and it is given by the expression:

$$TC = \frac{m_w \cdot c_w}{A(h_o + h_\infty)} \quad (14)$$

This quantity which determines the rate of exponential decay of wall heat flux involves the entire wall mass m_w and depends on the per unit area wall heat capacity $m_w c_w/A$ and the convective heat transfer coefficients.

2.2. The distributed parameter model

However, the idealized assumption of infinite thermal conductivity of wall material is not valid in practice. In homogeneous walls, the wall heat capacity is uniformly distributed over the wall thickness, which represents a uniformly distributed heat capacity across the thermal resistance of the heat flow path, normally to the wall plane. The space distribution of these two quantities may also be a complex function of the space coordinate as happens in composite walls. The combination of multiple layers of various structural materials and thermal insulation in thermal contact imposes significant variation and complex distribution of both, heat capacity and thermal resistance, owing to the difference between the thermophysical properties of materials involved, which may usually be significant. The relatively low thermal conductivity of most structural materials leads to the development of significant thermal resistance for most practical wall thicknesses and violation of the condition (3), so the system cannot any more be treated as a lumped parameter model. Assuming that a non-homogenous wall consists of n homogenous layers of uniform thermophysical properties and that each homogeneous layer i, $1 \le i \le n$, of thickness δ_i is split into a number of thin N_i slices of thickness Δx_i, a composite wall can typically be considered as a large number of N_w slices, $N_w = \sum_{i=1}^{n} N_i$ in thermal contact, with thermophysical properties ρ_i, c_i and k_i and a thickness of $\Delta x_i = \delta_i/N_i$, so as,

$$L = \sum_{i=1}^{n} \Delta x_i \cdot N_i. \quad (15)$$

As can be seen in Fig. 1b, each slice can typically be replaced by a T network with a lumped value of heat capacity $C_{is} = C_i/N_i$, with $C_i = \rho_i \cdot c_i \cdot \delta_i$, connected to the temperature node at its geometric centre of a representative temperature T_{is}. This capacitive element is connected to the slice boundaries through the two halves of the slice thermal resistance $r_{is} = R_i/(2N_i)$ and all T network slice elements, with parameters r_{is}, C_{is}, r_{is} are interconnected into a long chain of resistive and capacitive elements. The wall is bounded by its exterior and interior temperature nodes T_∞ and T_o, respectively, which are interconnected with the wall boundaries through the corresponding film resistances $R_\infty = 1/(h_\infty \cdot A)$ and $R_o = 1/(h_o \cdot A)$, respectively.

As the number of slices N_i increases, the thickness Δx_i and capacity C_{is} decrease and the discretised model tends to become identical to physical model with distributed parameters.

Under these conditions appreciably high temperature gradients are developed within the mass of the conductive wall medium during transient phenomena and the temperature field in the homogenous layer i of thickness δ_i of a composite wall with n homogeneous layers, $1 \le i \le n$, is governed by the one-dimensional transient Fourier equation,

$$\frac{\partial}{\partial x} \left[k_i \cdot \frac{\partial T_i(x,t)}{\partial x} \right] = \rho_i \cdot c_i \cdot \frac{\partial T_i(x,t)}{\partial t} \quad (16)$$

where ρ_i, c_i and k_i are the density, heat capacity and thermal conductivity of layer material.

It has been proposed that the time constant of a wall with distributed parameters can be derived by the investigation of its transient thermal response, under the effect of a step temperature change at a particular wall side [9]. The solution of Eq. (16) is derived numerically, under the initial condition of an isothermal wall and the following boundary conditions, corresponding to the heat balance at the ambient and room homogeneous layer surfaces, $i = 1$ and n, respectively:

$$k_1 \cdot \frac{\partial T_1(0,t)}{\partial x} + h_\infty [T_\infty(t) - T_1(0,t)] = 0 \tag{17}$$

$$k_n \cdot \frac{\partial T_n(\delta_n,t)}{\partial x} + h_o [T_n(\delta_n,t) - T_o(t)] = 0 \tag{18}$$

with the step function at the room side defined as,

$$T_0(t) = \begin{cases} 0, & \text{for} t < 0 \\ T_0, & \text{for} t \geq 0 \end{cases} \tag{19}$$

Based on the assumption of continuity at the surface boundaries of homogenous layers, the following condition of identical interfacial temperatures for the adjacent inner homogeneous layers should also be satisfied:

$$T_i(\delta_i,t) = T_{i+1}(0,t), \quad 1 \leq i < n \tag{20}$$

A real wall with distributed parameters exhibits an appreciably different transient thermal behavior as compared to the previously presented idealized lumped parameter model. Structural elements are continuums with scattered heat capacities and thermal resistances, the space distribution of which inhibits the participation of their whole heat capacity in the transient thermal processes, as happens in the case of the lumped parameter model. Therefore, the effective wall heat capacity denotes the fraction of the lumped heat capacity, which participates in a dynamic heat transfer process, owing to the effect of combined space distribution of heat capacity and thermal resistance across the heat flow path. This fraction can be considered as a dimensionless parameter, defined as the heat capacity ratio, so

$$\xi = \frac{(m_w c_w / A)_{\text{eff}}}{m_w c_w / A} \tag{21}$$

Therefore, according to (14) the effective heat capacity of a real wall with distributed heat capacity is calculated by,

$$\left(\frac{m_w \cdot c_w}{A} \right)_{\text{eff}} = \text{TC} \cdot (h_o + h_\infty) \tag{22}$$

which indicates that calculation of this significant quantity requires the evaluation of wall thermal time constant (TC), as calculated for the distributed system.

Owing to the efficiency and flexibility of numerical methods and their compatibility with contemporary powerful computational hardware, the long standing finite difference method was employed for the solution of Eq. (16).

Towards this aim the network node number, which depends on the corresponding number of slices and determines their thickness Δx_i, $1 \leq i \leq n$, and the time step of integration Δt were determined by splitting the time domain of integration t_d into a large number of p time increments Δt, so $t_d = p \cdot \Delta t$. The proper selection of Δx_i and Δt, being a trade off between desired accuracy and computational effort, was based on numerical experiment as was previously reported in [5].

Eqs. (16)–(18) were translated to a set of simultaneous algebraic equations, corresponding to each inner and boundary node of the thermal network using an inherently stable implicit finite difference scheme, as is also discussed in greater detail in [19]. The Laasonen and Crank–Nickolson approximations where employed leading both to almost identical results, as is also discussed in [7,19].

The derived solutions representing the exponential wall response of a particular wall design to the specific step temperature change were employed for the evaluation of the wall thermal time constant corresponding to a particular wall side.

3. Results and discussion

The results from the present investigation are based on extensive simulations of the transient thermal behavior of appropriately selected wall group samples, under properly defined step function excitations. The effect of a fixed, uniformly distributed heat capacity on walls of different widths although of a constant thermal resistance was first investigated, followed by subsequent investigations aiming at its influence on walls with a decreasing thermal resistance. The effect of the particular thermal insulation location was investigated next, in the case it is installed at the room, ambient or wall plane of symmetry, in a group of walls of fixed heat capacity although of a varying thermal resistance. Finally the influence of thermal insulation layer was examined, as it successively moves from the room to the ambient side of wall of a fixed heat capacity and thermal resistance. In all cases and for reasons of symmetry the convective heat transfer coefficients were assumed to be uniform at both wall boundaries, $h_o = h_\infty = 12$ W/m^2 K.

3.1. The uniform distribution of heat capacity

The effect of uniform distribution of a fixed wall heat capacity and thermal resistance over the width L was first investigated on the effective wall heat capacity. Towards this aim three wall groups A–C, with uniformly distributed thermophysical properties and different widths L, were selected. The first group includes the walls A_1–A_3 with $L = 0.18$–0.06 m, the second B_1–B_4 with $L = 0.24$–0.06 m and the third C_1–C_5 with $L = 0.3$–0.06 m, respectively, as shown in Fig. 2a. It was assumed that the reference walls A_1, B_1 and C_1 correspond to concrete with thermophysical properties $\rho_c = 2300$ kg/m^3, $c_c = 880$ J/(kg K) and $k_c = 1.2$ W/(m K). The fixed wall thermal resistance and heat capacity are $RA = 0.15$ m^2 K/W and $(m_w c_w/A) = 364.3$ kJ/(m^2 K) for group A, $RA = 0.20$ m^2 K/W and $(m_w c_w/A) = 485.7$ kJ/(m^2 K) for

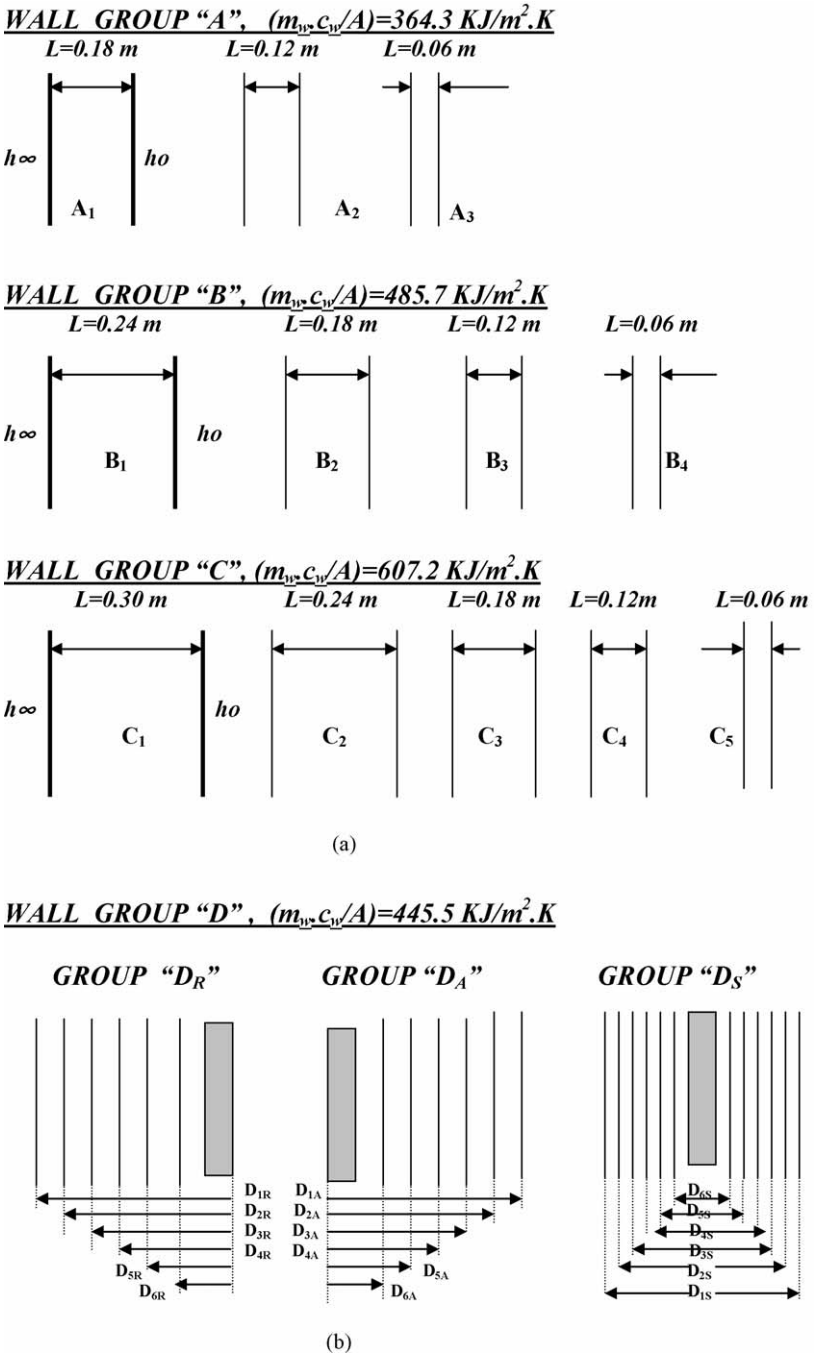

Fig. 2. (a) The walls A_1–A_3, B_1–B_4 and C_1–C_5 of the wall groups A–C with $m_w \cdot c_w/A$ = 364.3, 485.7 and 607.2 kJ/(m^2 K). (b) The composite walls D_{1S}–D_{6S}, D_{1R}–D_{6R} and D_{1A}–D_{6A} corresponding to $m_w \cdot c_w/A$ = 445.5 kJ/(m^2 K) with the insulation layer location at the plane of symmetry, room and ambient sides, respectively.

group B and $RA = 0.25$ m^2 K/W and $(m_w c_w/A) = 607.2$ kJ/(m^2 K) for group C, something which made necessary the appropriate selection of density and thermal conductivity of walls A_2–A_3, B_2–B_4 and C_2–C_5 as shown in the second and third column of Table 1, keeping the value of specific heat capacity c_c = 880 J/(kg K) constant. The time constant of walls was then evaluated and the derived results were employed for the calculation of the effective wall heat capacity from (22). Identical time constant and effective heat capacity for all the walls in each group were derived, owing to the fact that a fixed heat capacity is uniformly distributed over the fixed thermal resistance of the selected wall samples. This shows that for a fixed wall heat capacity, its effective heat capacity depends only on the uniformly distributed thermal resistance, irrespective of their width *L*.

The effect of a uniform heat capacity distribution across a varying wall thermal resistance was next investigated. Towards this aim the wall density in each group A–C was allowed to vary appropriately as shown in the second column of Table 1, although both the thermal conductivity and specific heat

Table 1
Modified thermophysical properties for the walls in groups A–C, with c_c = 880 J/(kg K)

Wall designation	ρ_c (kg/m^3)	k_c (W/(m K))
A_1, B_1, C_1	2300	1.20
A_2	3450	0.80
A_3	6900	0.40
B_2	3066.6	0.90
B_3	4600	0.60
B_4	9200	0.30
C_2	2875	0.96
C_3	3833.3	0.72
C_4	5750	0.48
C_5	11500	0.24

capacity kept constant, equal to 1.2 W/(m K) and 880 J/(kg K), respectively. Owing to this, the walls in the groups A–C are now of a uniform heat capacity although of a decreasing thermal resistance, respectively, to their width L.

Their effective heat capacity was calculated as before, through the evaluation of their time constant. Derived results are shown in Fig. 3, in which the effective per unit area heat capacity $(m_w c_w/A)_{eff}$ and time constant (TC) in solid and broken lines, respectively, are plotted against the wall thermal resistance. In the same plot the derived values of $(m_w c_w/A)_{eff}$ and TC corresponding to the lumped parameter model are comparatively shown for the zero abscissa value of thermal resistance. According to derived results it can be seen that for each wall group A–C, a decrease of wall thermal resistance leads to an increase of the effective wall heat capacity and this effect is more pronounced for the walls of higher heat capacity. As the thermal resistance decreases, the effective heat capacity increases closely to the value of the zero thermal resistance lumped parameter model.

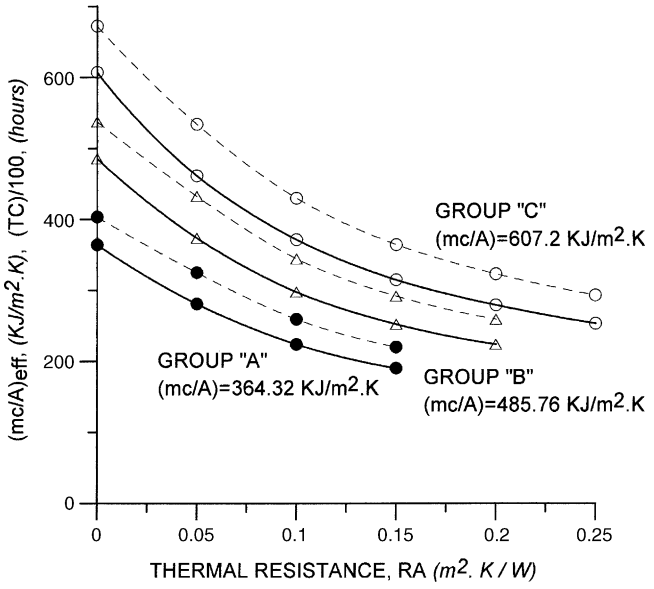

Fig. 3. The effective wall heat capacity (solid lines) and time constant (broken lines) plotted as a function of the thermal resistance for the homogenous wall groups A, B and C corresponding to 364.32, 485.76 and 607.2 kJ/(m^2 K), respectively.

It can also be seen that both effective heat capacity and effective heat capacity ratio ξ are strongly affected by the wall thickness which determines its thermal resistance. As also derived from the plotted results, the heat capacity ratio ξ decreases from its maximum unity value, corresponding to the lumped parameter model, to the value of about 0.52, 0.46 and 0.42 for the wall groups A, B and C, as the thermal resistance increases up to the value of 0.15, 0.2 and 0.25 m^2 K/W, respectively. This reveals the fundamental effect of thermal resistance to control the wall heat capacity and allows the definition of the effective wall heat capacity, which is a quantity related to the distribution of heat capacity across a heat flow path of a finite thermal resistance.

3.2. The effect of non-uniform space distribution of heat capacity and thermal resistance

Towards this aim three wall groups D_{iR}, D_{iA} and D_{iS}, $1 \leq i \leq 6$, of a fixed $(m_w c_w/A)$ = 445.53 kJ/(m^2 K) were developed as shown in Fig. 2b, consisting of six composite walls each. The walls in each group consist of a thermal insulation layer of a thermal conductivity and thickness of 0.04 W/m K and 0.06 m respectively, and a different number of brick layers of the same thickness, with a density which was allowed to vary appropriately, as shown in Table 2, to ensure a uniform wall heat capacity. The thermal insulation layer in the group D_R is placed at the room side, while an increasing number of brick layers are stacked at the opposite side. Therefore, as shown in Fig. 2b, the wall D_{1R} of L = 0.42 m consists of six brick layers of ρ_b = 1400 kg/m^3, c_b = 880 J/(kg K) and k_b = 0.6 W/(m K) stacked at the opposite side of the thermal insulation layer, while D_{6R} corresponds to a wall of L = 0.12 m, which consists of a thermal insulation and a brick layer of an appropriately selected density to ensure that $(m_w c_w/A)$ = 445.53 kJ/(m^2 K). The thermal insulation of the walls in the groups D_A and D_S is located at the ambient side and at the plane of symmetry, respectively, as also is shown in Fig. 2b. Therefore, the walls D_{3R}, D_{3A} and D_{3S} are of a uniform heat capacity, width and thermal resistance corresponding to $(m_w c_w/A)$ = 445.53 kJ/(m^2 K), L = 0.30 m and RA = 1.9 m^2 K/W, respectively, although they only differ on the insulation layer location which is at the room side, ambient side and wall mid-plane, respectively.

Following the same procedure, the time constant and the effective heat capacity of the developed walls with the three different brick and insulation layer configurations were calculated and the results are plotted in Fig. 4. According to

Table 2
Modified thermophysical properties for the walls in group D, with c_b = 880 J/(kg K) and k_b = 0.6 W/(m K)

Wall designation	ρ_b (kg/m^3)
D_{1S}, D_{1R}, D_{1A}	1400
D_{2S}, D_{2R}, D_{2A}	1680
D_{3S}, D_{3R}, D_{3A}	2100
D_{4S}, D_{4R}, D_{4A}	2800
D_{5S}, D_{5R}, D_{5A}	4200
D_{6S}, D_{6R}, D_{6A}	8400

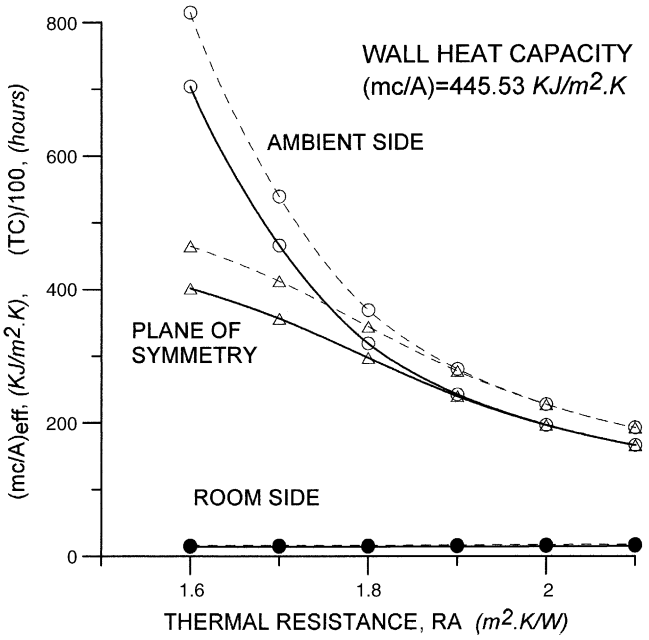

Fig. 4. The effective wall heat capacity (solid lines) and time constant (broken lines) plotted as a function of the thermal resistance for the multilayer walls of groups D_S, D_R and D_A with $m_w \cdot c_w/A = 445.5$ kJ/(m^2 K), corresponding to thermal insulation location at the wall plane of symmetry, room and ambient sides, respectively.

the derived results the thermal insulation layer location, which determines the space distribution of thermal resistance and heat capacity at a direction perpendicular to the wall plane, strongly influences the effective wall heat capacity. The space distribution of heat capacity and thermal resistance for a wall of $L = 0.42$ m corresponding to $RA = 2.1$ m^2 K/W, with a thermal insulation layer installed at its plane of symmetry, leads to an effective heat capacity of about 200 kJ/(m^2 K) which increases to more than 400 kJ/(m^2 K) when the same wall heat capacity is distributed over the width of $L = 0.12$ m corresponding to the lower thermal resistance of $RA = 1.6$ m^2 K/W. This corresponds to an increase of the effective heat capacity ratio ξ, by a factor of approximately 2.3. The influence is far stronger with the thermal insulation placed at the ambient wall side, something which leads to a corresponding effective heat capacity increase from the same initial value of about 200 kJ/(m^2 K) to the value of about 700 kJ/(m^2 K), for the same range of thermal resistance variation. This corresponds to a remarkably higher increase of the effective heat capacity ratio ξ, up to a value of 3.6. When however the thermal insulation layer is installed at the room side, there is a negligible effect on the effective wall heat capacity and ratio ξ, which remains practically constant, irrespective of the wall thermal resistance.

According to the derived results, an effective control of the wall heat capacity could be possible, either by varying the wall width or the thermal insulation layer location. A substantial increase of effective heat capacity may be possible by the distribution of wall heat capacity over a layer of a limited thickness in a thermal contact with the thermal insulation layer, only when it is installed at the ambient side. In this case large specific heat capacity and thermal conductivity materials favor the development of high effective wall heat capacity. It is derived that the effective heat capacity of a composite wall is a complex function of insulation layer thickness and location, which determines the wall layer configuration as well as the thermophysical properties of the wall materials involved. These influence strongly the wall thermal resistance, heat capacity and its space distribution, which are parameters determining the wall heat capacity imbalance in respect of the wall plane of symmetry.

Attempting finally to isolate the specific effect of the thermal insulation layer location irrespective of wall heat capacity and thermal resistance, the following three wall groups E, F and G of seven, five and three walls, corresponding to a width of $L = 0.42$, 0.30 and 0.18 m, respectively, were developed as shown in Fig. 5. These wall groups are comprised of a thermal insulation layer and six, four and two brick layers, respectively, each, of a 0.06 m thickness in a thermal contact. The walls in each group are developed by the different configurations of insulation and brick layers, so the thermal insulation layer for the walls E_1 and E_7, F_1 and F_5, and G_1 and G_3 is placed at the ambient and room wall sides, respectively. The heat capacity and thermal resistance of the so developed seven E_1–E_7, five F_1–F_5 and three G_1–G_3 walls correspond to $(m_w c_w/A) = 445.5$, 297.7 and 149.8 kJ/(m^2 K) and $RA = 2.1$, 1.9 and 1.7 m^2 K/W, respectively. The wall pairs E_i and $E_{j-(i-1)}$ for $j = 7$, F_i and $F_{j-(i-1)}$ for $j = 5$ and G_i and $G_{j-(i-1)}$ for $j = 3$ with $1 \leq i \leq j$ are symmetric in respect of wall mid-plane, with $TC_{F,E_i} = TC_{R,E_{j-(i-1)}}$.

The effective heat capacity and time constant of the 15 walls were calculated and the results were plotted and fitted with solid and broken lines, respectively, against the distance between thermal insulation layer boundary facing the room side and ambient wall surface, as shown in Fig. 6.

Referring to the wall group E with $(m_w c_w/A) = 445.53$ kJ/(m^2 K), it can be seen that as the thermal insulation layer moves from the room to the wall mid-plane, their effective heat capacity increases sharply up to a value of about 165 kJ/(m^2 K) and remains unchanged as the layer moves further from wall mid-plane to ambient side. A qualitatively similar behavior is exhibited by the walls in groups F and G with heat capacities of 297.69 and 149.85 kJ/(m^2 K), respectively, as shown in the same plot. Although very small effective heat capacities are developed when the insulation layer is at the room side, they are rapidly increasing closely to the constant value of about 160 and 157 kJ/(m^2 K) as the thermal insulation layer moves towards ambient side.

It would be worth noting that these values correspond to an effective heat capacity ratio ξ of 0.372, 0.547 and 1.051 for the walls E_1, F_1 and G_1, respectively, which are far lower than the values developed by the wall D_{6A} in Fig. 4, of the same heat capacity, which is about 1.6. This is attributed to the fact that although walls E_1 and D_{6A} are of identical heat capacity, the heat capacity of the wall E_1 is distributed over a thermal resistance of 2.1 m^2 K/W, which corresponds to the width of $L = 0.42$ m while in the wall D_{6A} of the same heat capacity, it is distributed over the substantially lower thermal resistance of 1.60 m^2 K/W which corresponds to a wall width of 0.12 m.

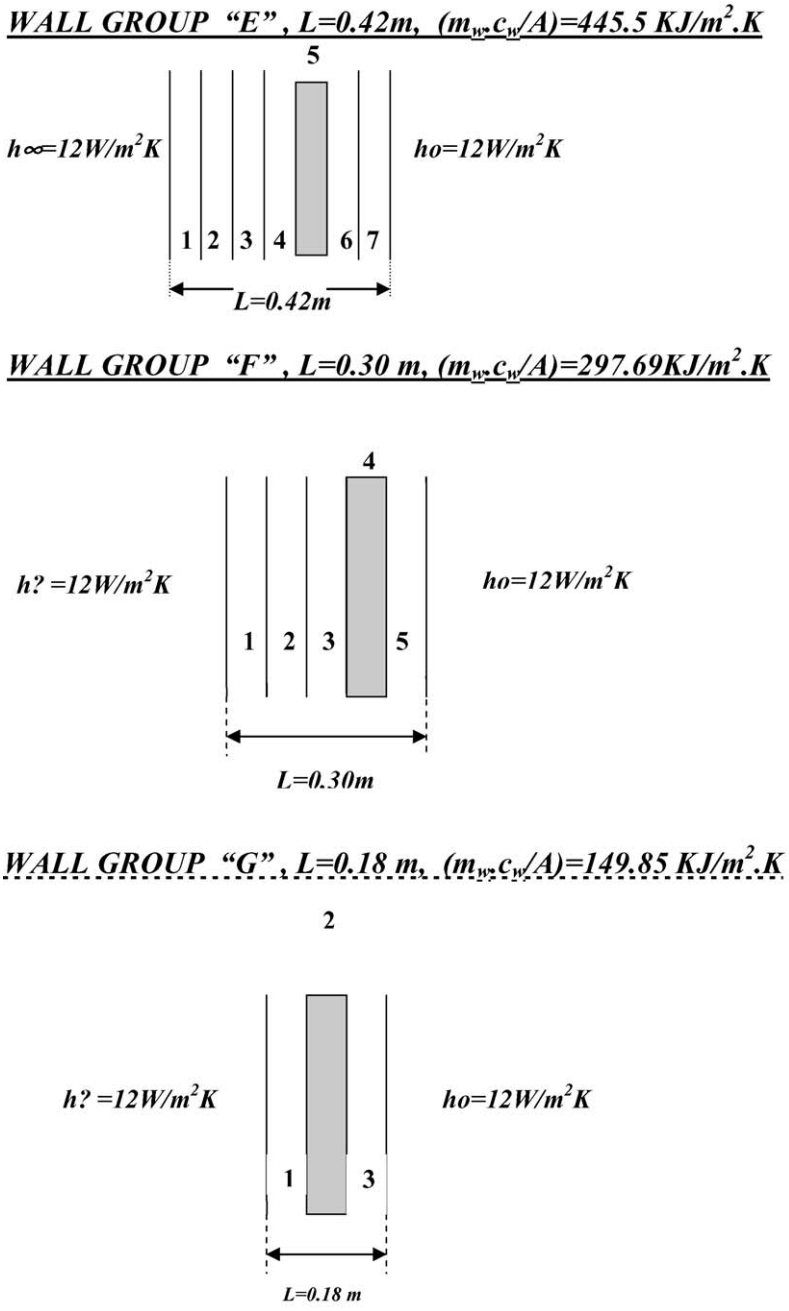

Fig. 5. The walls E_1–E_7, F_1–F_5 and G_1–G_3 with per unit area heat capacity of $m_w \cdot c_w/A$ = 445.5, 297.69 and 149.85 kJ/(m^2 K) and thickness of L = 0.42, 0.30 and 0.18 m, respectively.

4. Implications on the building thermal behavior

The dynamic behavior of structures is not only related to their thermal insulation efficiency, but also on their heat capacity, which is the contribution of the distributed mass within the building and represents the heat capacity of the building envelope and the internal mass. This consists of the heat capacity of interior partitions, room air as well as of the heat capacity of temporary mass, which is mostly unpredictable as it is associated to the specific use of the building. However, owing to the mass distribution and the weak thermal coupling between various heat capacity components through complex heat transfer conductances, only a fraction of the total building heat capacity participates in dynamic heat exchange processes and this represents the effective heat capacity of the building. Effective heat capacity is an important quantity, strongly related to the building thermal time constant, which determines the thermal inertia of structures, their heat storage capability and their thermal stability. The thermal stability is related to the ability of the building to suppress efficiently interior temperature swings and improves as the amplitude ratio of the harmonically time varying room to ambient air temperature decreases [11].

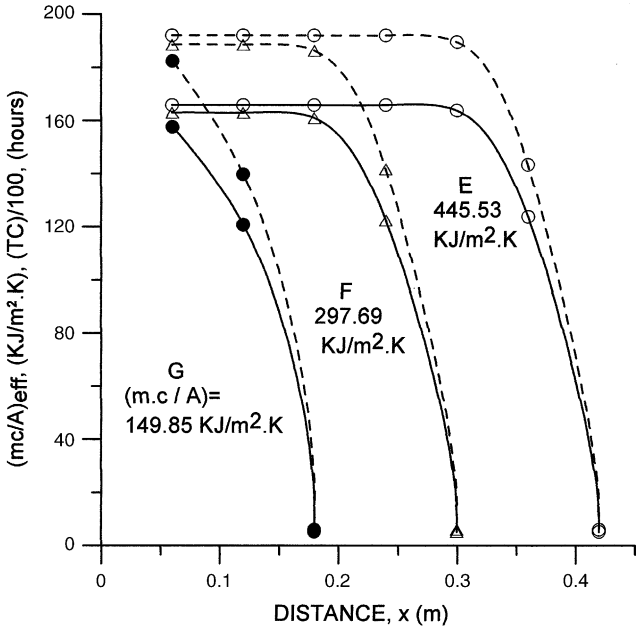

Fig. 6. The effective wall heat capacity (solid lines) and time constant (broken lines) plotted as a function of the distance between the thermal insulation layer boundary facing room side and the ambient wall surface, for the multilayer walls E_1–E_7, F_1–F_5 and G_1–G_3, with per unit area heat capacity of $m_w \cdot c_w/A = 445.5$, 297.69 and 149.85 kJ/(m^2 K) and thickness of $L = 0.42$, 0.30 and 0.18 m, respectively.

According to earlier investigations [7], it was derived that the wall design affects considerably the building thermal behavior by suppressing efficiently wall heat fluxes and temperature fluctuations, as well as phasing out peaking thermal loads. Aiming to carry out first order investigations on the influence of the effective wall heat capacity to the time constant of a simplified building model, a negligible temporary heat capacity and a small internal mass as compared to the heat capacity of the building envelope were assumed, something which is valid for heavy building envelope structures with lightweight or movable partitions.

The so developed simplified model represents a single space building in the form of a rectangular box with dimensions 3.0 m × 3.0 m × 3.0 m and identical walls. Assuming that the walls are completely shaded, they are subjected to the influence of harmonically time-varying temperature of the ambient air, which surrounds its boundary walls. Therefore, for the purpose of this first order approach prediction of the time dependent room air temperature and owing to the full symmetry of the system, it is possible to assume one-dimensional conduction heat exchange between room air and environment as also proposed in [11].

The development of the simple model was based, as previously, on the numerical solution of the one-dimensional diffusion equation (16) for the non-homogeneous wall using the finite difference method, under the appropriate boundary condition (17) for the ambient side, with $T_\infty(t)$ representing now the diurnal variation of ambient temperature for a typical winter day corresponding to 20 January. This is expressed with a good accuracy by the following simple, single term harmonic function:

$$T_\infty(t) = \bar{T} + T_m \cdot \cos\left(\frac{2\pi}{24} \cdot t - \varphi\right) \tag{23}$$

with average and amplitude values $\bar{T} = 8.62\ ^\circ$C and $T_m = 3.68\ ^\circ$C, respectively, and a phase angle of $\varphi = 225^\circ$ as also discussed in [19].

Assuming that the room heat capacity represents the whole indoor air mass m_a, the following simple heat balance equation can be used as the room air boundary condition:

$$Q_n(t) - h_o \cdot A_w \cdot [T_o(t) - T(L,t)] = m_a \cdot c_a \cdot \frac{\partial T_o(t)}{\partial t} \tag{24}$$

The quantity $Q_n(t)$ in the previous expression represents the room net heat input which is the contribution of the room heat gain owing to the operation of the terminal heater and infiltration–ventilation losses. Assuming for the purpose of this approach that $Q_n(t) = 0$, the so developed finite difference computer model is employed to carry out first order investigations concerning the fundamental influences of building envelope thermal resistance, heat capacity distribution and insulation layer configuration on the time constant and effective heat capacity of the whole structure.

The walls of the room envelope were assumed to be similar to those of wall group G with constant heat capacity and thermal resistance of $m_w c_w/A = 149.85$ kJ/(m^2 K) and $RA = 1.7$ m^2 K/W, respectively, although of a vastly different thermal time constant and effective heat capacity. The calculations were carried out for the cooling down period of an initially isothermal structure at $T_i(t) = 20\ ^\circ$C and the simulation time domain was extended up to eight successive typical winter days.

Indicative results are shown in Fig. 7 in which the room temperature is plotted against time, for the three different walls G_1–G_3. It is derived that the use of the wall G_3 with the minimum effective heat capacity leads to the rapid reduction of time dependent room temperature, which fluctuates remarkably over its average value with the same period although a different phase angle with ambient temperature. Although the use of the wall G_3 leads to a rapid cooling of room air, practically within the first 50 h owing to the effect of thermal insulation which is installed at the room side, the walls G_2 and G_1 lead to a far slower cooling with a simultaneous strong suppression of the room temperature swing. This is a highly desirable effect since it strongly improves the thermal stability of the room as more heat capacity is available between thermal insulation and room space. As derived from the exponential envelope of the three cooling curves, the use of walls G_3, G_2 and G_1 leads to an increasing building thermal time constant of about 4.75, 20.00 and 31.25 h, respectively, something which underlines the importance of thermal insulation layer location in composite wall structures and confirms the favorable effects of external insulation on continuously conditioned massive buildings.

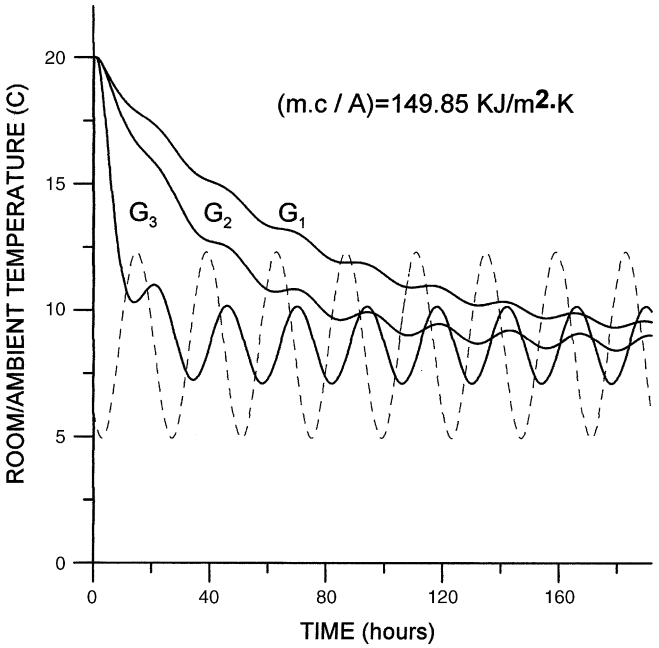

Fig. 7. Prediction of room air temperature (solid lines) as a function of time during the cooling down period for external walls of the group G corresponding to $m_w \cdot c_w/A = 149.85$ kJ/(m^2 K), with the thermal insulation layer installed at the ambient side (G_1), wall mid-plane (G_2) and room side (G_3). Broken line represents the time varying ambient temperature.

5. Conclusions

The aim of the present work was to underline the effects and to parametrically investigate the relative influences of significant physical parameters, which affect the transient thermal behavior of the building envelope. The building envelope can generally be considered as a continuum with a random space distribution of heat capacity and a thermal resistance which is distinctively different as compared to the lumped parameter model, corresponding to an idealized medium of respective concentrated in space parameters. The presented analysis has allowed the development of the fundamental relationship between wall thermal time constant and effective per unit area heat capacity, which physically represents the fraction of the lumped heat capacity that participates in a transient thermal process. This fraction representing the dimensionless ratio of effective to lumped heat capacity was defined as the effective heat capacity ratio. According to results from extensive simulations it was found that the effective heat capacity of homogeneous walls, as derived for step temperature change excitations at the room side, depends strongly on the combined space distribution effects of heat capacity and thermal resistance. Reduction of thermal resistance leads to a significant increase of the effective heat capacity and the heat capacity ratio up to the unity value, something which corresponds to the idealized lumped capacity systems. However, the effective heat capacity was found to be much more sensitive to the effect of layer configuration in non-homogeneous wall systems.

While the effect of a thermal insulation layer at the room side leads generally to very small effective heat capacity values, its effect at the opposite ambient wall side leads to an increase of effective heat capacity for walls of a fixed heat capacity and thermal resistance. This increase appears to be far stronger with the possibility of restriction of the fixed wall heat capacity over a heat flow path of a lower thermal resistance. The derived results, referring to the structural elements of the building envelope, were employed to investigate the corresponding implications on the effective heat capacity and the thermal stability of a simplified building model. Indicative results are showing that the effect of using large effective heat capacity walls with the thermal insulation at the ambient side not only leads to a substantial increase of the building thermal time constant but also improves the thermal stability of the structure when exposed to harmonically time varying excitations by substantial suppression of room temperature swings.

References

[1] R.J. Duffin, G. Knowels, A passive wall design to minimize building temperature swings, Solar Energy 33 (6) (1984) 543–549.
[2] M.G. Davies, Wall transient heat flow using time-domain analysis, Building and Environment 32 (1997) 427–446.
[3] T. Weber, G. Johannesson, An optimized *RC* network for thermally activated building components, Building and Environment 40 (1) (2005) 1–14.
[4] R. Yumrutas, M. Unsal, M. Kanoglu, Periodic solution of transient heat flow through multilayer walls and flat roofs by complex finite Fourier transform technique, Building and Environment 40 (2005) 1117–1125.
[5] P.T. Tsilingiris, On the transient thermal behavior of structural walls—the combined effect of time-varying solar radiation and ambient temperature, Renewable Energy 27 (2002) 319–336.
[6] S.A. Al-Sanea, Thermal performance of building roof elements, Building and Environment 37 (2002) 665–675.
[7] P.T. Tsilingiris, Thermal flywheel effects on time varying conduction heat transfer through structural walls, Energy and Buildings 35 (2003) 1037–1047.
[8] J.E. Christian, J. Kosny, Thermal performance and wall ratings, ASHRAE Journal (March) (1996) 56–65.
[9] P.T. Tsilingiris, On the thermal time constant of structural walls, Applied Thermal Engineering 24 (2004) 743–757.
[10] E. Kossecka, J. Kosny, Relations between structural and dynamic thermal characteristics of building walls, in: Proceedings of International Symposium of CIB W67 "Energy and Mass Flow in the Life Cycle of Buildings", Vienna, August 4–10, (1996), pp. 627–632.
[11] E. Kossecka, J. Kosny, Influence of insulation configuration on heating and cooling loads in a continuously used building, Energy and Buildings 34 (2002) 321–331.
[12] R.C. Sonderegger, Diagnostic tests determining the thermal response of a house, Transactions of ASHRAE (Part 1) (1978) 691–702.
[13] P.S. Gujral, R.J. Clark, D.M. Burch, Transient thermal behaviour of an externally insulated massive building, Transactions of ASHRAE 86 (Part 2) (1980) 521–534.
[14] J.E. Janssen, Application of building thermal-resistance measurement techniques, Transactions of ASHRAE 88 (Part 1) (1982) 713–731.
[15] R.R. Crawford, J.E. Woods, A method for deriving a dynamic system model from actual building performance data, Transactions of ASHRAE 91 (Part 2B) (1985) 1859–1874.
[16] F. Haghighat, M. Chandrashekar, System-theoretic models for building thermal analysis, Transactions of ASME, Journal of Solar Energy Engineering 109 (1987) 79–88.

[17] A.K. Athienitis, H.F. Sullivan, K.G.T. Hollands, Analytical model, sensitivity analysis and algorithm for temperature swings in direct gain rooms, Solar Energy 36 (4) (1986) 303–312.
[18] K.A. Antonopoulos, E.P. Koronaki, Effect of mass on the time constant and thermal delay of buildings, International Journal of Energy Research 24 (2000) 391–402.
[19] P.T. Tsilingiris, The influence of heat capacity and its spatial distribution on the transient wall thermal behavior under the effect of harmonically time-varying driving forces, Building and Environment 41 (2006) 590–601.
[20] F.P. Incropera, D.P. DeWitt, Fundamentals of Heat and Mass Transfer, second ed., John Wiley & Sons, NY, 1985.